

Analytical method for the out-of-plane buckling of the jib system with middle strut

T.F. Wang, N.L. Lu and P. Lan*

School of Mechatronics Engineering, Harbin Institute of Technology, Harbin 150001, P.R. China

(Received February 18, 2015, Revised March 08, 2016, Accepted July 01, 2016)

Abstract. The jib system with middle strut is widely used to achieve the large arm length in the large scale tower crane and the deployability in the mobile construction crane. In this paper, an analytical solution for the out-of-plane buckling of the jib system with middle strut is proposed. To obtain the analytical expression of the buckling characteristic equation, the method of differential equation was adopted by establishing the bending and torsional differential equation of the jib system under the instability critical state. Compared with the numerical solutions of the finite element software ANSYS, the analytical results in this work agree well with them. Therefore, the correctness of the results in this work can be confirmed. Then the influences of the lateral stiffness of the cable fixed joint, the dip angle of the strut, the inertia moment of the strut, and the horizontal position of the cable fixed joint on the out-of-plane buckling behavior of the jib system were investigated.

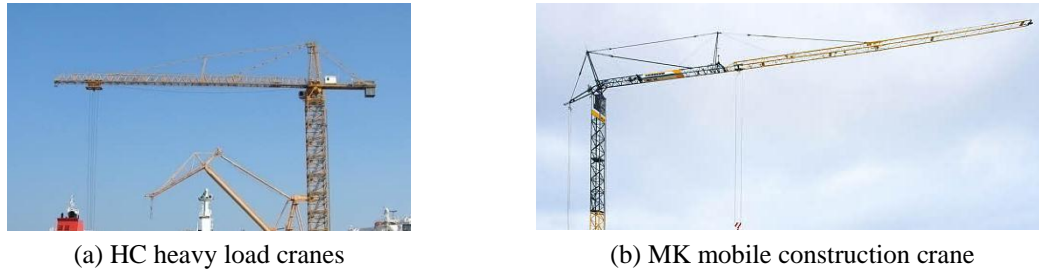
Keywords: tower crane; jib system with middle strut; out-of-plane buckling; analytical solution; method of differential equation

1. Introduction

In the tension structure, the cable tension can improve the stress condition of the structure and make full use of the individual material properties (Hosozawa *et al.* 1999). Meanwhile, the stiffness and the stability of the structure are improved significantly by the tension system comprised of tensile cables and struts. Because of these notable advantages, the practical application of tension structure in the construction has grown rapidly in recent thirty years, especially the application in the large span spatial structure (Wakefield 1999, Hangai and Wu 1999). Also, the concept of tension structure is extended to the tower crane jib system to realize the large arm length. A large number of tower crane manufacturers adopt such jib system with middle strut between two jibs in their tower crane products, such as the HC heavy load cranes of Liebherr. The jib system of HC series is shown as Fig. 1(a).

Interestingly, the jib system with middle strut is also widely applied in the mobile construction crane to realize the deployability and fast overhead assembly. As shown in Fig. 1(b), in the mobile construction crane, the automatic assembly and erecting of the tower crane is realized through the deployable jib system and the telescopic lattice tower. Correspondingly, the wide application of the jib system with middle strut in the construction crane makes it warranted to investigate the

*Corresponding author, Associate Professor, E-mail: lan_p@sina.com



(a) HC heavy load cranes

(b) MK mobile construction crane

Fig. 1 The jib system with middle strut in Liebherr tower crane products

buckling of the jib system with middle strut.

While a number of related researches about tension structure in various forms such as the beam string structure have been carried out by many scholars, few researches on its application in crane jib can be found. Wu (2008) and Xue and Liu (2010) presented the analytical solution for the lateral buckling of the beam string structure with the method of differential equation and the Ritz-method. El-Ghazaly and Al-Khaiat (1995) conducted the study on the out-of-plane stability of the guyed transmission tower based on the minimum potential energy principle. De Araujo *et al.* (2008) and Saito and Wadee (2009) made the investigations on the buckling of the stayed column via the experimental method and the Rayleigh-Ritz method. Yoo and Choi (2009) researched the buckling of the girder and tower members in steel cable-stayed bridges. In conclusion, the existing researches are mainly about the beam string structure, the guyed tower, the stayed column and the cable-stayed bridge excluding the jib system with middle strut.

The jib system with a middle strut belongs to tension structure, and its structural analysis is complex because of the high nonlinearity. The key to the stability analysis is how to process the action of the flexible cable tension. As for the normal crane jib/boom with the guyed cables/rods, large amount of work has been done. Li *et al.* (2015), Wang *et al.* (2015) and Wen *et al.* (2013) studied nonlinear stability of the flexible boom system equipped in giant cranes, stability of the jib system with auxiliary bracing used in crawler cranes, and stability of the double-rod jib applied in tower cranes with horizontal arm. Compared with the buckling mode of the aforementioned jib with guyed cables/rods, that of the jib system with middle strut is different due to the existence of the strut. Specifically, when the jib system buckles in the lateral plane, there occurs side sway combined with torsional deformation. Therefore, it's more complex to analyze the stability of the jib system with middle strut. Although lots of efforts have been put on the buckling analysis of the normal jib system, there is a lack of study on the out-of-plane stability analysis of the jib system with middle strut.

It should be noted that the out-of-plane buckling is easier to occur compared with the in-plane buckling for the jib system. The jib system is generally taken as the two-point or multi-point simply supported structure in the lifting plane. By contrast, the jib system is normally processed as cantilever structure with one end clamped and the other end free out of the lifting plane. As the critical load of the cantilever structure is much lower than that of multi-point simply supported structure, the out-of-plane buckling is easier to occur. In addition, the out-of-plane buckling will occur suddenly once the lifting load reaches the critical value without any symptoms, which makes the out-of-plane buckling more harmful than the in-plane buckling. Accordingly, greater emphasis has been placed on the out-of-plane stability, which is also the topic of the paper.

The main purpose of this paper is to propose an analytical method for the out-of-plane buckling

of the jib system with middle strut. Initially, the accurate stability analysis model considering the lateral flexibility of the cable fixed joint was built. Then, the bending and torsional deformation differential equations of the jib system under the buckling critical state were established. By introducing the boundary conditions and deformation compatibility equations, the analytical expression of the buckling characteristic equation was obtained, and the analytical solution obtained was compared with the numerical solution presented by the widely used finite element software ANSYS. Following the verification, a range of influential parameters were investigated to study their effects on the buckling behavior of the jib system.

2. Buckling characteristic equation of the jib system

Generally, there are two jib forms, i.e., the lattice jib and the solid web one. And the lattice jib can be equivalent to the solid web jib with some proper methods. Accordingly, there are two steps to analyze the stability of the lattice jib system in the practical application. Firstly, the lattice jib is equivalent to the solid web one. Then, analytical or numerical method are adopted to analyze the equivalent system including solid web beam, bar and tension cable. Thus, the time consuming modeling of the real spacial lattice can be avoided, which is significant to check the jib system stability quickly in the practical engineering. As the paper focus on the analytical method for the stability analysis, i.e., the second step, the equivalent solid web jib system instead of the real lattice jib is taken as the research object in both the analytical method and the following numerical verification

The lattice model and the equivalent solid web model of the jib system with middle strut are shown as Figs. 2(a) and (b). The jib system is composed of two hinged jibs and the tension system, which comprises the guyed cables and the middle strut between jibs. Note that the guyed cable is fixed at the top of tower head.

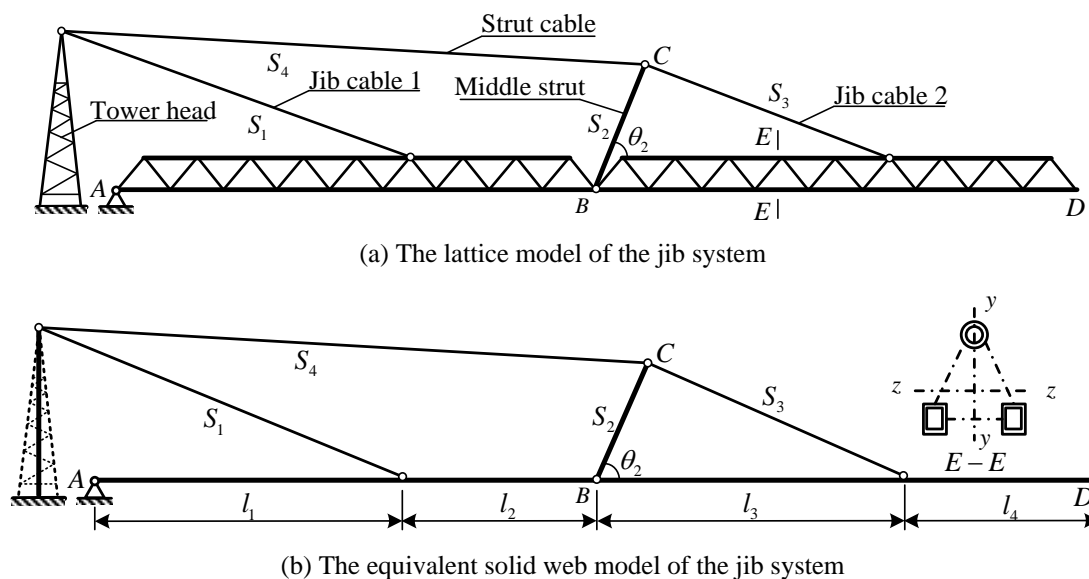


Fig. 2 The analysis model of the jib system

The structure parameters of the tension system are as follows: the length and the dip angle of the strut are S_2 and θ_2 , the length of the two jib cables are S_1 and S_3 and the length of the strut cable is S_4 . As shown in Fig. 2(b), the length of the jib segments separated by the hanging points and the hinge joint are l_i ($i = 1 \sim 4$).

Note that the influence of the eccentricity of the hanging points and the hinge joints with respect to the centroidal axis of the jib on the out-of-plane stability of the jib is very slight (Lu *et al.* 2014). Thus, during the equivalent process from the lattice model to the solid web model, the hanging points and the hinge joints can be moved directly to the centroidal axis. The out-of-plane buckling of the jib belongs to the bifurcation buckling. As the main focus of the study is the stability behavior of the jib system, namely the critical buckling load or the effective length factor of the beam-bar system. Additionally, in practical engineering, the distributed dead weight of the crane jib has a slight influence on the out-of-plane stability of the jib system. Therefore, it is reasonable to neglect the dead weight of the crane jib to simplify the subsequent derivation.

As shown in Fig. 2, the jib system is a statically determinate structure. When the lifting weight is applied on jib 1, i.e., the AB segment, only jib cable 1 is tensioned. In contrast, when the lifting weight is applied on jib 2, i.e., the BD segment, all the cables are tensioned, and the strut is compressed. Therefore, the stability of the jib system should be discussed depending on the radius of the lifting weight.

2.1 The buckling characteristic equation with lifting weight applied on jib 1

When the lifting weight is applied on jib 1, only jib cable 1 is tensioned. As a result, the jib system degenerated to the jib guyed by a single cable. The out-of-plane buckling mode thereof is shown as Fig. 3.

Note that the stiffness of the tower head is relatively small compared to that of the jib. Thus, the lateral flexibility of the cable fixed joint should be taken into account during the out-of-plane buckling analysis. As shown in Fig. 3, there occurs lateral displacement δ_0 at the cable fixed joint when the jib buckles. The buckling analysis of the jib with single guyed cable has been made by Lan *et al.* (2014). Nevertheless, for the sake of completeness, the stability analysis of the jib system in the case of single guyed cable is elaborated briefly.

As shown in Fig. 4, a_1 is the length of the horizontal projection of jib cable 1. Build the coordinate system with the jib axial direction as x axis direction and the hinge joint of the jib as the origin to analyze the stability of the jib.

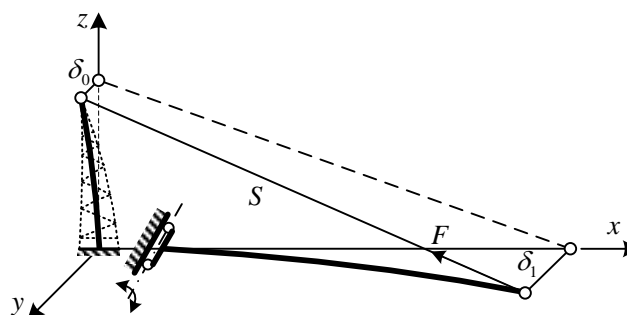


Fig. 3 The out-of-plane buckling mode of the jib tensioned by a single cable

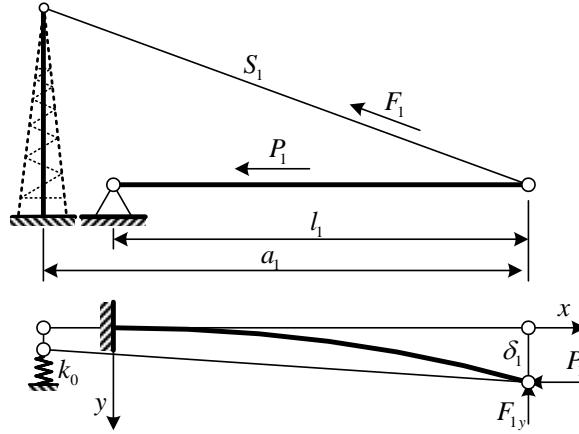


Fig. 4 The out-of-plane buckling analysis of jib with single guyed cable

Introduce the lateral stiffness k_0 to represent the lateral restraint on the guyed cable imposed by the cable fixed joint. For conciseness, a dimensionless factor ξ is introduced to relate the lateral stiffness of the fixed joint with that of the cantilever beam with length l_1 at the free end. Thus, one can obtain $k_0 = \xi \cdot (EI / l_1^3)$. It is easy to get the out-of-plane buckling characteristic equation by establishing the bending differential equation of the jib in the coordinate system. The buckling characteristic equation of the jib system with lifting weight applied on jib 1 is

$$\tan \omega_1 l_1 = \omega_1 l_1 \left[1 - \frac{a_1}{l_1} - \frac{(\omega_1 l_1)^2}{\xi} \right] \quad (1)$$

Where the intermediate value $\omega_1 = \sqrt{P_1 / EI_1}$ and P_1 is the axial force of jib 1. Let $\xi \rightarrow \infty$, namely the lateral stiffness of the cable fixed joint k_0 tends to be infinite. The cable is then laterally clamped at the cable fixed joint, Eq. (1) degenerates to the equation proposed by Timoshenko and Gere (1961).

2.2 The buckling characteristic equation with lifting weight applied on jib 2

When the lifting weight is applied on jib 2, all the guyed cables are tensioned, and the middle strut is compressed. Accordingly, the buckling analysis of the jib system becomes more complicated. The structure parameters for the buckling analysis are defined in Fig. 5.

As shown in Fig. 5, a_i ($i = 1 \sim 4$) are the horizontal projection length of the cables/strut S_i and a_0 is the horizontal distance between the cable fixed joint and the root hinge joint of jib 1. To get unified expression, denote $a_0 = l_0$. The buckling mode of the jib system is shown as Fig. 6. When the structure buckles in the lateral plane, there appear lateral displacements δ_i ($i = 1 \sim 4$) at the hanging points and the ends of the strut. As mentioned in the previous section, the lateral flexibility of the cable fixed joint should be considered, so there occurs a lateral displacement δ_0 at the fixed joint. The tension of the guyed cables and the compression of the strut are denoted as F_i ($i = 1 \sim 4$).

Establish the coordinate system $O_1 X_1 Y_1 Z_1$ with the jib axial direction as x axis direction and the hinge joint of the jib 1 as the origin. Similarly, establish the coordinate system $O_2 X_2 Y_2 Z_2$ and

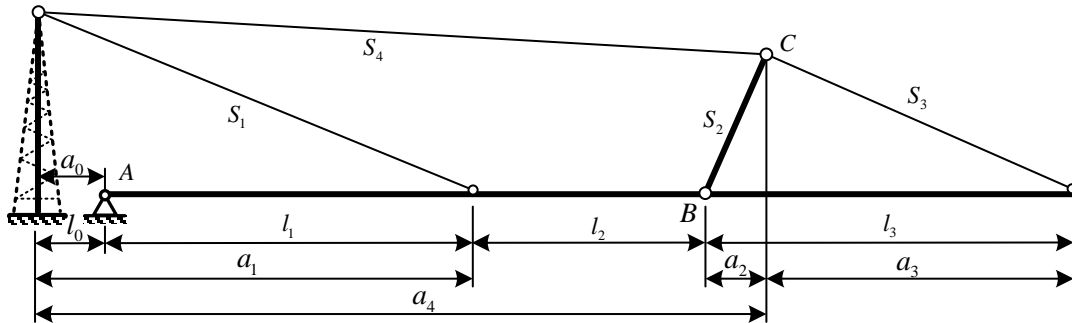


Fig. 5 The structure parameters of the jib system for the buckling analysis

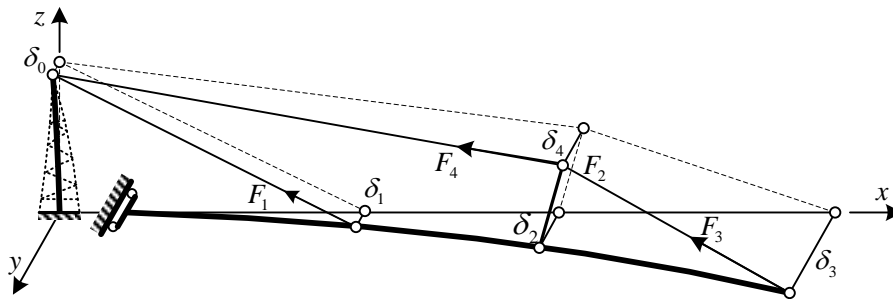


Fig. 6 The out-of-plane buckling mode of the jib system

$O_3X_3Y_3Z_3$ with the hanging point of jib 1 and the hinge joint of jib 2 as the origin. And the coordinate systems $O_iX_iY_iZ_i$ ($i = 1 \sim 3$) share the same x axis direction. Then establish the strut coordinate system $O_4X_4Y_4Z_4$ with the strut axial direction as x axis direction and the hinge joint of jib 2 as the origin. The coordinate systems $O_iX_iY_iZ_i$ ($i = 1 \sim 4$) are shown in Fig. 7(a).

Under the buckling critical state, establish the deformation differential equation of the jib segments and the strut in the corresponding coordinate systems. In Fig. 7, the component of the cable tensions and strut compression in jib axial direction are N_i ($i = 1 \sim 4$) and the lateral components thereof are F_{iy} ($i = 1 \sim 4$). In the analysis of jib segment 1 and jib segment 2, which is shown as Fig. 7(a), the triangle structure consisting of the strut, jib segment 3 and jib cable 2 is considered as a single member. The analysis of jib segment 3 and the strut are shown as Fig. 7(b) and Fig. 7(c).

The lateral component of the cable tensions and the strut compression F_{iy} ($i = 1 \sim 4$) are

$$\begin{cases} F_{1y} = [(\delta_1 - \delta_0) / S_1] \cdot F_1 & F_{2y} = F_{4y} - F_{3y} \\ F_{3y} = [(\delta_3 - \delta_4) / S_3] \cdot F_3 & F_{4y} = [(\delta_4 - \delta_0) / S_4] \cdot F_4 \end{cases} \quad (2)$$

The component of the cable tensions and strut compression in jib axial direction are $N_i = (a_i / S_i) \cdot F_i$, and it is easy to get $N_4 = N_2 + N_3$. As the lateral component of the cable tensions and the strut compression F_{iy} can be linearly expressed by the lateral displacements δ_i , they can be treated as the elastic recovery forces. And thus, the equivalent elastic supports at the hanging points and the hinge joint of jib 2 are introduced to simplify the derivation. The corresponding equivalent lateral

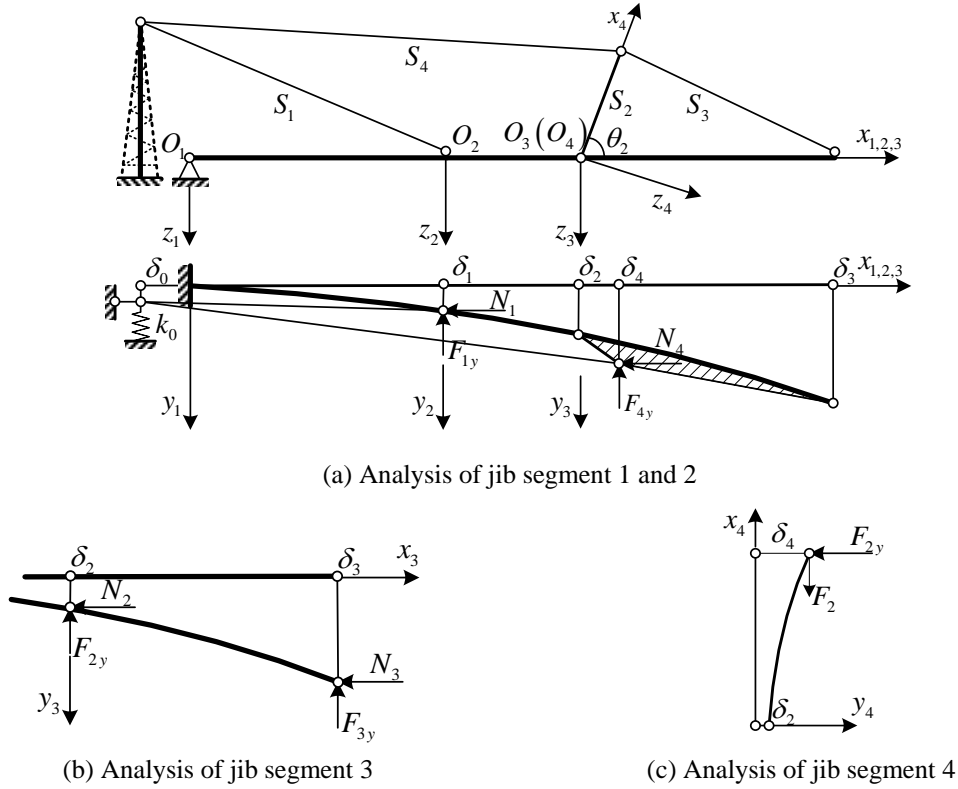


Fig. 7 The force analysis of the jib system under the buckling critical state

stiffness is $k_i = N_i / a_i$. As a result, $N_i = k_i a_i$ and the lateral forces F_{iy} can be expressed as

$$\begin{cases} F_{1y} = k_1 (\delta_1 - \delta_0) & F_{2y} = F_{4y} - F_{3y} \\ F_{3y} = k_3 (\delta_3 - \delta_4) & F_{4y} = k_4 (\delta_4 - \delta_0) \end{cases} \quad (3)$$

As the lateral stiffness of the cable fixed joint is k_0 , the corresponding lateral recovery force associated with the lateral displacement δ_0 at the cable fixed joint can be obtained as $F_{0y} = k_0 \delta_0$. And the equilibrium equation at the cable fixed joint in the lateral direction is

$$F_{0y} = F_{1y} + F_{4y} \quad (4)$$

The lateral displacement δ_0 can be eliminated by substituting Eq. (3) into Eq. (4) and then the linear expression of the lateral forces F_{iy} ($i = 1 \sim 4$) can be **get** with respect to the lateral displacements δ_i ($i = 1 \sim 4$).

$$\begin{cases} F_{1y} = \eta_{11} \delta_1 + \eta_{14} \delta_4 & F_{2y} = \eta_{41} \delta_1 - k_3 \delta_3 + (k_3 + \eta_{44}) \delta_4 \\ F_{3y} = k_3 (\delta_3 - \delta_4) & F_{4y} = \eta_{41} \delta_1 + \eta_{44} \delta_4 \end{cases} \quad (5)$$

Where the expressions of the intermediate stiffness factor η are as follows

$$\begin{cases} \eta_{11} = \frac{k_1(k_0 + k_4)}{k_0 + k_1 + k_4} & \eta_{14} = -\frac{k_1 k_4}{k_0 + k_1 + k_4} \\ \eta_{41} = -\frac{k_1 k_4}{k_0 + k_1 + k_4} & \eta_{44} = \frac{k_4(k_0 + k_1)}{k_0 + k_1 + k_4} \end{cases} \quad (6)$$

The inertia moment of the jib segments and the strut are I_i ($i = 1 \sim 4$), and Young's Modulus is E . Establish the bending deformation differential equations of the jib segments and the strut in the corresponding coordinate system as follows

$$\begin{cases} EI_1 y_1'' = N_1(\delta_1 - y_1) + N_4(\delta_4 - y_1) - F_{1y}(l_1 - x_1) - F_{4y}(a_4 - a_0 - x_1) \\ EI_2 y_2'' = N_4(\delta_4 - y_2) - F_{4y}(a_4 - a_1 - x_2) \\ EI_3 y_3'' = N_3(\delta_3 - y_3) - F_{3y}(l_3 - x_3) \\ EI_4 y_4'' = F_2(\delta_4 - y_4) - F_{2y}(S_2 - x_4) \end{cases} \quad (7)$$

Define the axial compression of the three jib segments as P_i ($i = 1 \sim 3$) and that of the strut as P_4 , and thus

$$\begin{cases} P_1 = N_1 + N_2 + N_3 & P_3 = N_3 \\ P_2 = N_2 + N_3 & P_4 = F_2 \end{cases} \quad (8)$$

Substitute the expression of the lateral force F_{iy} into the differential equation and recall the definition of the equivalent lateral stiffness k_i , the differential equations can be written as

$$\begin{cases} EI_1 y_1'' + P_1 y_1 = \frac{k_1 \delta_1 + k_4 \delta_4}{k_0 + k_1 + k_4} \cdot [P_1 + k_0(a_0 + x_1)] \\ EI_2 y_2'' + P_2 y_2 = (a_1 + x_2) \cdot k_4 \delta_4 + \frac{k_1 \delta_1 + k_4 \delta_4}{k_0 + k_1 + k_4} \cdot k_4(a_4 - a_1 - x_2) \\ EI_3 y_3'' + P_3 y_3 = -(a_2 - x_3) \cdot k_3 \delta_3 + (l_3 - x_3) \cdot k_3 \delta_4 \\ EI_4 y_4'' + P_4 y_4 = (S_2 - x_4)(k_3 \delta_3 - \eta_{41} \delta_1) + [F_2 - (k_3 + \eta_{44})(S_2 - x_4)] \delta_4 \end{cases} \quad (9)$$

The general solutions of the differential equations Eq. (9) are

$$\begin{cases} y_1 = A_1 \cos \omega_1 x_1 + B_1 \sin \omega_1 x_1 + \frac{k_1 \delta_1 + k_4 \delta_4}{k_0 + k_1 + k_4} \cdot \left[1 + \frac{\xi}{(\omega_1 l_1)^2} \cdot \frac{a_0 + x_1}{l_1} \right] \\ y_2 = A_2 \cos \omega_2 x_2 + B_2 \sin \omega_2 x_2 + \frac{a_1 + x_2}{a_4} \delta_4 + \frac{k_1 \delta_1 + k_4 \delta_4}{k_0 + k_1 + k_4} \cdot \frac{a_4 - a_1 - x_2}{a_4} \\ y_3 = A_3 \cos \omega_3 x_3 + B_3 \sin \omega_3 x_3 - \frac{a_2 - x_3}{a_3} \delta_3 + \frac{l_3 - x_3}{a_3} \delta_4 \\ y_4 = A_4 \cos \omega_4 x_4 + B_4 \sin \omega_4 x_4 + \frac{S_2 - x_4}{F_2} (k_3 \delta_3 - \eta_{41} \delta_1) + \left[1 - \frac{k_3 + \eta_{44}}{F_2} (S_2 - x_4) \right] \delta_4 \end{cases} \quad (10)$$

Where the intermediate variable $\omega_i = \sqrt{P_i/EI_i}$. And a dimensionless factor ξ is introduced to relate the lateral stiffness of the fixed joint k_0 to that of the cantilever beam with length l_1 at its free end. That means $k_0 = \xi \cdot (EI_1 / l_1^3)$.

The linear expression of unknowns A_i and B_i with respect to the lateral displacements δ_i can be obtained by using the boundary conditions and deformation compatibility equations. Denote the transformation matrix as \mathbf{R}_i , and thus $\{A_i \ B_i\} = \mathbf{R}_i \cdot \boldsymbol{\delta}$. Where $\boldsymbol{\delta}$ is the lateral displacement vector, name $\boldsymbol{\delta} = \{\delta_1 \ \delta_2 \ \delta_3 \ \delta_4\}^T$. The boundary conditions and deformation compatibility equations of the jib system are as follows

$$\begin{cases} x_1 = 0 & y_1 = 0 & y_1' = 0 \\ x_2 = 0 & x_1 = l_1 & y_2 = y_1 & y_2' = y_1' \\ x_3 = 0 & x_2 = l_2 & y_3 = y_2 & y_3' = y_2' \\ x_4 = 0 & y_4 = \delta_2 & y_4' = \mathbf{m} \cdot \boldsymbol{\delta} \end{cases} \quad (11)$$

Recall the deflection curve equation Eq. (10), the expressions of the transformation matrices \mathbf{R}_i ($i = 1 \sim 4$) are obtained as

$$\begin{cases} \mathbf{R}_1 = \frac{1}{k_0 + k_1 + k_4} \cdot \begin{bmatrix} k_1 \left[1 + \frac{\xi}{(\omega_1 l_1)^2} \cdot \frac{a_0}{l_1} \right] & 0 & 0 & k_4 \left[1 + \frac{\xi}{(\omega_1 l_1)^2} \cdot \frac{a_0}{l_1} \right] \\ \frac{k_1 \cdot \xi}{(\omega_1 l_1)^3} & 0 & 0 & \frac{k_4 \cdot \xi}{(\omega_1 l_1)^3} \end{bmatrix} \\ \mathbf{R}_2 = \mathbf{T}_2 \cdot \mathbf{R}_1 + \frac{1}{k_0 + k_1 + k_4} \cdot \mathbf{U}_2 \\ \mathbf{R}_3 = \mathbf{T}_3 \cdot \mathbf{R}_2 + \mathbf{U}_3 \\ \mathbf{R}_4 = \begin{bmatrix} \frac{\eta_{41}}{k_2} & 1 & -\frac{k_3}{k_2} & -\left(1 - \frac{k_3 + \eta_{44}}{k_2} \right) \\ \frac{\mathbf{m}(1) - \eta_{41} / F_2}{\omega_4} & \frac{\mathbf{m}(2)}{\omega_4} & \frac{\mathbf{m}(3) + k_3 / F_2}{\omega_4} & \frac{\mathbf{m}(4) - (k_3 + \eta_{44}) / F_2}{\omega_4} \end{bmatrix} \end{cases} \quad (12)$$

Where \mathbf{T}_2 and \mathbf{U}_2 in the expression of the transformation matrix \mathbf{R}_2 are the intermediate matrices. The expressions thereof are as follows.

$$\begin{cases} \mathbf{T}_2 = \frac{1}{\omega_2} \cdot \begin{bmatrix} \omega_2 \cos \omega_1 l_1 & \omega_2 \sin \omega_1 l_1 \\ -\omega_1 \sin \omega_1 l_1 & \omega_1 \cos \omega_1 l_1 \end{bmatrix} \\ \mathbf{U}_2 = \frac{1}{\omega_2} \cdot \begin{bmatrix} \omega_2 k_1 \left[\frac{\xi}{(\omega_1 l_1)^2} \cdot \frac{a_1}{l_1} + \frac{a_1}{a_4} \right] & 0 & 0 & \omega_2 \left[\frac{\xi}{(\omega_1 l_1)^2} \cdot \frac{k_4 a_1}{l_1} - (k_0 + k_1) \cdot \frac{a_1}{a_4} \right] \\ k_1 \left[\frac{\xi}{(\omega_1 l_1)^2} \cdot \frac{1}{l_1} + \frac{1}{a_4} \right] & 0 & 0 & \frac{\xi}{(\omega_1 l_1)^2} \cdot \frac{k_4}{l_1} - (k_0 + k_1) \cdot \frac{1}{a_4} \end{bmatrix} \end{cases} \quad (13)$$

Similarly, the intermediate matrices \mathbf{T}_3 and \mathbf{U}_3 in the expression of the transformation matrix \mathbf{R}_3 are expressed as follows.

$$\begin{cases} \mathbf{T}_3 = \frac{1}{\omega_3} \cdot \begin{bmatrix} \omega_3 \cos \omega_2 l_2 & \omega_3 \sin \omega_2 l_2 \\ -\omega_2 \sin \omega_2 l_2 & \omega_2 \cos \omega_2 l_2 \end{bmatrix} \\ \mathbf{U}_3 = \frac{1}{\omega_3} \cdot \begin{bmatrix} \omega_3 \cdot \frac{a_2}{a_4} \cdot \frac{k_1}{k_0 + k_1 + k_4} & 0 & \omega_3 \cdot \frac{a_2}{a_3} & -\omega_3 \cdot \left[\frac{a_2}{a_3} + \frac{a_2}{a_4} \cdot \frac{k_0 + k_1}{k_0 + k_1 + k_4} \right] \\ -\frac{1}{a_4} \cdot \frac{k_1}{k_0 + k_1 + k_4} & 0 & -\frac{1}{a_3} & \frac{1}{a_3} + \frac{1}{a_4} \cdot \frac{k_0 + k_1}{k_0 + k_1 + k_4} \end{bmatrix} \end{cases} \quad (14)$$

The compatibility between the strut and the jib at the hinge joint should be introduced to deduce the linear expression of the unknowns A_4 , B_4 with respect to the lateral displacements δ_i . As mentioned in Eq. (11), to get the transformation matrix \mathbf{R}_4 , let $y_4 = \delta_2$ and $y'_4 = \mathbf{m} \cdot \boldsymbol{\delta}$ at $x_4 = 0$. Where \mathbf{m} is the slope vector and it can be obtained by establishing the compatibility equation and the torsional deformation differential equation. The detailed process is as follows. Define φ as the torsion angle of the jib under the buckling critical state. As the torsion angle is small, it follows that

$$y'_4(0) = y'_3(0) \cos \theta_2 + \varphi \sin \theta_2 \quad (15)$$

Let $y'_3(0) = \mathbf{p} \cdot \boldsymbol{\delta}$. Recall the deflection curve equation of jib segment 3, it can be obtained that

$$\mathbf{p} = \{0 \quad \omega_3\} \cdot \mathbf{R}_3 + \{0 \quad 0 \quad 1/a_3 \quad -1/a_3\} \quad (16)$$

There occurs a torsional angle φ for the jib under the tension of the strut cable. The shear modulus is G and the torsional moment of inertia is I_p . Then the torsional deformation differential equation can be written as

$$GI_p \frac{d\varphi}{dx} = -F_{2y} S_2 \sin \theta_2 + F_2 \sin \theta_2 (\delta_4 - \delta_2) \quad (17)$$

Let $\varphi = \mathbf{q} \cdot \boldsymbol{\delta}$. Integrate Eq. (17), and thus the intermediate vector \mathbf{q} is got as

$$\mathbf{q} = \frac{(l_1 + l_2) \sin \theta_2}{GI_p} \cdot \{-\eta_{41} S_2 \quad -F_2 \quad k_3 S_2 \quad F_2 - (k_3 + \eta_{44}) S_2\} \quad (18)$$

Combining the equations above, the slope vector \mathbf{m} can be expressed as

$$\mathbf{m} = \mathbf{p} \cdot \cos \theta_2 + \mathbf{q} \cdot \sin \theta_2 \quad (19)$$

Following the solution of the transformation matrices \mathbf{R}_i ($i = 1 \sim 4$), the linear equations with respect to the lateral displacements δ_i ($i = 1 \sim 4$) are obtained by using the remaining boundary conditions.

$$\begin{cases} x_2 = 0 & y_2 = \delta_1 & A_2 + \frac{a_1}{a_4} \delta_4 + \frac{k_1 \delta_1 + k_4 \delta_4}{k_0 + k_1 + k_4} \cdot \frac{a_4 - a_1}{a_4} = \delta_1 \\ x_3 = 0 & y_3 = \delta_2 & A_3 - \frac{a_2}{a_3} \delta_3 + \frac{l_3}{a_3} \delta_4 = \delta_2 \\ x_3 = l_3 & y_3 = \delta_3 & A_3 \cos \omega_3 l_3 + B_3 \sin \omega_3 l_3 = 0 \\ x_4 = S_2 & y_4 = \delta_4 & A_4 \cos \omega_4 S_2 + B_4 \sin \omega_4 S_2 = 0 \end{cases} \quad (20)$$

Substitute the transformation matrices \mathbf{R}_i into Eq. (20), the linear equations Eq. (20) can be written in the matrix form $\mathbf{K} \cdot \boldsymbol{\delta} = \mathbf{0}$ as

$$\mathbf{K} \cdot \boldsymbol{\delta} = \begin{bmatrix} \mathbf{v}_{\mathbf{kl}} \\ \{1 \ 0\} \cdot \mathbf{R}_3 + \{0 \ -1 \ -a_2/a_3 \ l_3/a_3\} \\ \{\cos \omega_3 l_3 \ \sin \omega_3 l_3\} \cdot \mathbf{R}_3 \\ \{\cos \omega_4 S_2 \ \sin \omega_4 S_2\} \cdot \mathbf{R}_4 \end{bmatrix} \cdot \begin{Bmatrix} \delta_1 \\ \delta_2 \\ \delta_3 \\ \delta_4 \end{Bmatrix} = \mathbf{0} \quad (21)$$

Where the first row vector of the coefficient matrix $\mathbf{v}_{\mathbf{kl}}$ is

$$\mathbf{v}_{\mathbf{kl}} = \{1 \ 0\} \cdot \mathbf{R}_2 + \frac{1}{k_0 + k_1 + k_4} \cdot \left\{ - \left[(k_0 + k_4) + k_1 \frac{a_1}{a_4} \right] \ 0 \ 0 \ k_4 + \frac{a_1}{a_4} \cdot (k_0 + k_1) \right\} \quad (22)$$

It is required that the determinant of the coefficient matrix vanishes, if the buckling mode of the jib system exists, i.e., there exists a nontrivial solution for the linear equations about δ_i ($i = 1 \sim 4$). And thus, one can obtain that the out-of-plane buckling characteristic equation of the jib system $|K| = 0$ as follows.

$$\begin{vmatrix} \mathbf{v}_{\mathbf{kl}} \\ \{1 \ 0\} \cdot \mathbf{R}_3 + \{0 \ -1 \ -a_2/a_3 \ l_3/a_3\} \\ \{\cos \omega_3 l_3 \ \sin \omega_3 l_3\} \cdot \mathbf{R}_3 \\ \{\cos \omega_4 S_2 \ \sin \omega_4 S_2\} \cdot \mathbf{R}_4 \end{vmatrix} = 0 \quad (23)$$

The buckling characteristic equation Eq. (23) is a transcendental equation with respect to the component of the cable tensions and the strut compression in jib axial direction N_i ($i = 1 \sim 4$), the strut compression F_2 and the intermediate variables ω_i ($i = 1 \sim 4$). As all the aforementioned variables are functions of lifting weight, it is easy to get that the buckling characteristic equation is in reality a single-unknown equation with respect to the lifting weight. When the equation Eq. (23) holds, the lifting weight reaches the critical value Q_{cr} , the jib system buckles in the out-of-plane.

Given a certain radius, it is easy to get the proportional relation between F_i and N_i . The critical compression of one jib segment can be taken as the unknown. The critical compression can be written as $P_{icr} = \omega_i^2 E I_i$. And the dimensionless effective length factor is obtained as $\mu_i = \pi / \omega_i l_i$. The critical compressions of the other jib segments can easily get from the solved critical compression according to the proportion relation. In conclusion, the critical compression P_{icr} is obtained from the buckling characteristic equation. And one should note that the critical compression P_{icr} changes with the lifting radius r .

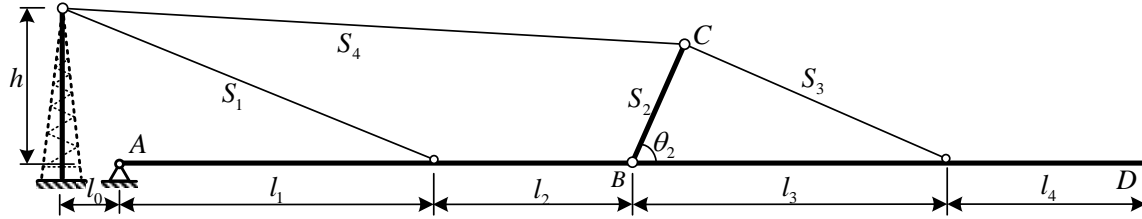


Fig. 8 The jib system of ST-160 tower crane

Table 1 The values of the structure parameters

Parameter	Value/m	Parameter	Value/m	Parameter	Value/ $\times 10^{-2} m^4$
l_1	25	l	80	$I_i (i = 1\sim 3)$	3.774
l_2	15	l_0	0.95	I_4	0.600
l_3	25	h	12.984	I_p	8.303
l_4	15	S_2	12	-	-

3. Numerical example

Take ST80-160 tower crane as an example to verify the analytical method proposed in this paper. The jib system of the tower crane is shown as Fig. 8.

The full length of the jib system is l and the dip angle of the strut is $\theta_2 = 60^\circ$. The values of the other structure parameters are listed in Table 1.

Establish the model in the general finite element software ANSYS to verify the analytical solution. The version of ANSYS used in the research is 12.0. In ANSYS, beam44 and link10 are used to simulate the jib and the guyed cable. It should be noted that the rotational stiffness should be released at the hinge joint and the link element should be set tension-only. The spring-damper element combin14 is used to simulate the lateral flexibility of the cable fixed joint.

As there is a determinate proportional relation among the critical axial compressions P_{icr} , one can just take the critical compression of jib segment 1 to conduct the comparison. To further simplify the comparison, the effective length factor μ_1 is chosen as the comparison item.

As elaborated in the previous section, the buckling characteristic equations are Eqs. (1) and (23) for the cases of the lifting weight applied on jib 1 and jib 2. It is noteworthy that the critical compression is unrelated to the radius when the lifting weight is applied on the first jib, and this case has already been covered in detail by Lan *et al.* (2014). Therefore, the study focuses on the second case, namely the lifting load applied on jib 2.

It should be pointed out that the lateral stiffness of the cable fixed joint supported by the tower head depends on many factors such as the tower head structure form, the structure dimension and the loading condition. The stability analysis is conducted only after the dimensionless lateral stiffness factor ζ is fixed. Generally, the range of the lateral stiffness factor ζ for the normal tower crane is 10~100. And the lateral stiffness factor for the tower crane ST80-160 used in the numerical example is $\zeta = 19.98$, which is approximately 20. The corresponding result is shown in Table 2. Besides the case of ST80-160, other three cases with ζ equal to 1, 5 and 10000 are analyzed in Table 2 to show the effectiveness of the method. The comparison between the

Table 2 The comparison between the analytical solution and the numerical solution on μ_1

Radius/m	$\xi = 1$			$\xi = 5$		
	Analytical μ_1	ANSYS μ_1	Error%	Analytical μ_1	ANSYS μ_1	Error%
≤ 40	1.792794	1.792794	0.00	1.519636	1.519636	0.00
44	1.874225	1.874226	0.00	1.579926	1.579926	0.00
52	2.054679	2.054679	0.00	1.736151	1.736150	0.00
60	2.223194	2.223195	0.00	1.896668	1.896666	0.00
68	2.364200	2.364201	0.00	2.031735	2.031736	0.00
80	2.528287	2.528287	0.00	2.185932	2.185932	0.00
Radius/m	$\xi = 20$			$\xi = 10000$		
	Analytical μ_1	ANSYS μ_1	Error%	Analytical μ_1	ANSYS μ_1	Error%
≤ 40	1.282360	1.282360	0.00	1.038736	1.038736	0.00
44	1.340200	1.340199	0.00	1.120286	1.120283	0.00
52	1.527041	1.527040	0.00	1.403869	1.403870	0.00
60	1.721018	1.721018	0.00	1.635809	1.635808	0.00
68	1.872851	1.872850	0.00	1.800555	1.800555	0.00
80	2.037722	2.037721	0.00	1.972888	1.972888	0.00

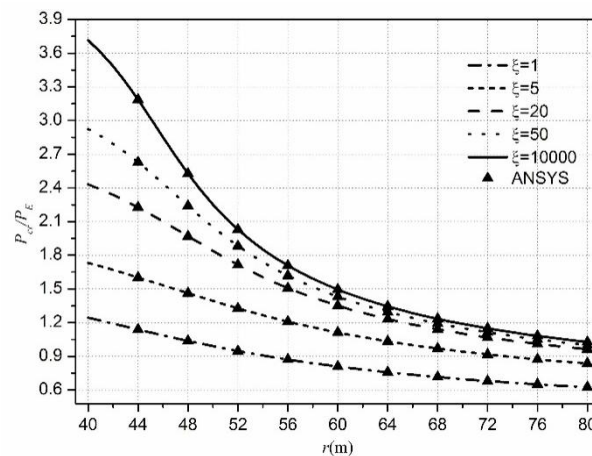


Fig. 9 The critical compression ratio along with the radius when the load is applied on jib 2

analytical solution and the ANSYS numerical solution on μ_1 associated with six various radiuses and four different lateral stiffness factors ξ is shown in Table 2.

As shown in Table 2, the analytical solution agrees well with the numerical solution presented by ANSYS. The analytical method proposed is verified.

When the lifting weight is applied on jib 2, the buckling load depends on the radius. To get a clear cognition of the relation, the change curve between the buckling load and the radius of the lifting weight is drawn as follows. Denote P_{cr} as the critical compression of jib segment 1 and P_E as the critical compression of a column with length l_1 in the case where its one end is clamped and

the other one is free. That implies $P_E = \pi^2 EI_1 / (2l_1)^2$. The relationship between the critical compression ratio P_{cr} / P_E and the radius under various lateral stiffness factors ζ of the cable fixed joint is shown in Fig. 9.

As shown in Fig. 9, the buckling load decreases with the increase of radius. Specially, for the case of $\zeta = 10000$ as shown in Fig. 9, the buckling load drops by 72% when the radius increases from 40 m to 80 m. In the case where the radius tends to be 40 m, the critical compression tends to be that of the jib with single cable tension. The reason is that the tension of cables and the compression of the strut tend to be zero except that of the jib 1 cable when the lifting weight approaches to the hinge joint of jib 2. And it should be noted that the buckling load has a slight change for different ζ when $\zeta > 20$. On the other hand, when $\zeta < 20$, the buckling load rises greatly with the increase of ζ . For instance, given a fixed radius $r = 64$ m as shown in Fig. 9, P_{cr} / P_E becomes 0.758, 1.033, 1.232, 1.296, and 1.345 when ζ is 1, 5, 20, 50 and 10000, respectively.

4. Parametric study

In this part, the influential factors on the out-of-plane stability of the jib system are studied. As is shown in the previous chapter, the buckling characteristic equation is a transcend equation. Thus, it is difficult to find out the influence of various parameters on the stability of the jib system directly. Given this circumstance, it is necessary to conduct the parametric study on the influential structure parameters including the lateral stiffness of the cable fixed joint, the dip angle of the strut, the inertia moment of the strut and the horizontal distance between the cable fixed joint and the hinge joint of jib 1. To simplify the study, for the parametric study, the lifting weight is fixed at the hanging point of jib 2, namely the radius is 65 m.

4.1 The lateral stiffness of the cable fixed joint

It is easy to know that the lateral stiffness of the cable fixed joint would influence the elements of the transformation matrix \mathbf{R}_i directly. In this way, the stiffness can influence the buckling characteristic equation $\text{Det}(\mathbf{K}) = 0$, and thus influence the buckling load of the jib system. To study the influence of the lateral stiffness of the cable fixed joint, set the variation range of the stiffness factor ζ as $\zeta = 1 \sim 100$. After introducing the Euler critical compression of a cantilever column with

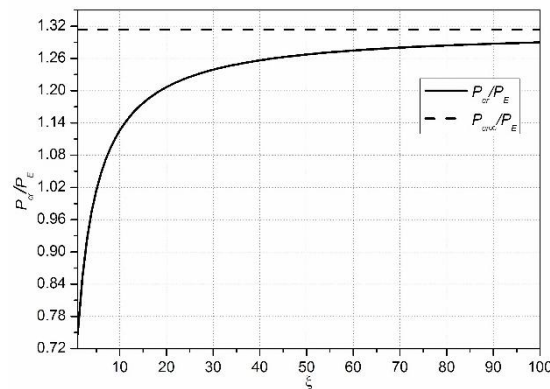


Fig. 10 The buckling load ratio along with the lateral stiffness factor

length l_1 as $P_E = \pi^2 EI_1 / (2l_1)^2$, the relationship between the buckling load ratio P_{cr} / P_E and the stiffness factor ξ is depicted as shown in Fig. 10.

It is obvious that the buckling load increases with the increase of the lateral stiffness factor in general. Specifically, there is a significant rise of the buckling load when the lateral stiffness factor is small. The buckling load increases by 40% during the growth of the stiffness factor from 1 to 20. And the growth of the buckling load becomes slight after the stiffness factor is bigger than 50. Specially, the critical compression reaches the extreme value when the stiffness factor tends to be infinite, which means the cable fixed joint is laterally clamped. From the change curve, it can be concluded that increasing the lateral stiffness of the cable fixed joint will greatly improve the buckling load of the jib system when the lateral stiffness is relatively small.

4.2 The dip angle of the strut

The existence of the strut leads to the torsional deformation of the jib system when the structure buckles. The dip angle of the strut influences the compatibility condition Eq. (15), and thus influences the buckling load of the jib system. Take the dip angle of the strut θ_2 as the study object. For the sake of simplification, the investigation is conducted in the case of clamped cable fixed joint, namely $\xi \rightarrow \infty$. Set the variation range of dip angle as $\theta_2 = 30^\circ \sim 150^\circ$. In a similar manner, the Euler critical compression $P_E = \pi^2 EI_1 / (2l_1)^2$ is introduced, and the relationship between the critical compression ratio P_{cr} / P_E and the dip angle of the strut is shown as Fig. 11.

As shown in Fig. 11, the buckling load increases gradually along with the dip angle with a peak at $\theta_2 = 90^\circ$. Then, there is a rapid fall for the buckling load with the increase of the dip angle. While the buckling load of the jib system decreases by 25% when the dip angle changes from 90° to 30° , the buckling load drops by 40% when the dip angle changes from 90° to 150° .

In conclusion, the buckling load reaches the maximum value when the dip angle is 90° . When the dip angle is acute angle, the buckling load is bigger compared with that when the dip angle is obtuse angle.

4.3 The inertia moment of the strut

The fourth linear equation with respect to the lateral displacements δ_i is obtained by establishing the bending differential equation of the strut and introducing the corresponding

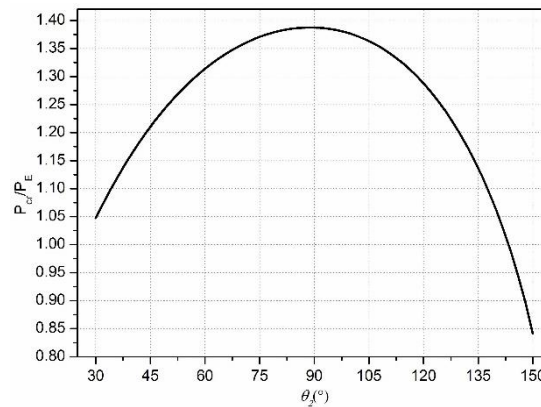


Fig. 11 The buckling load ratio along with the dip angle of the strut

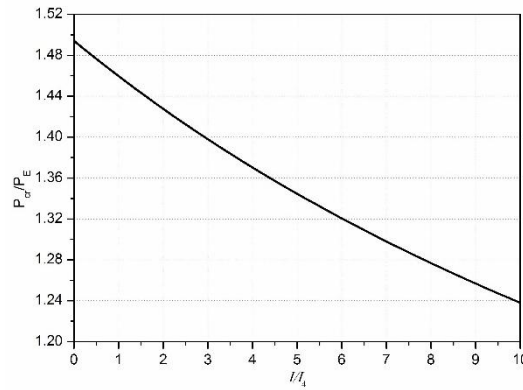


Fig. 12 The buckling load ratio along with inertia moment of the strut

boundary conditions. The inertia moment of the strut would influence the buckling characteristic equation of the jib system $\text{Det}(\mathbf{K}) = 0$ by influencing the fourth row of the coefficient matrix \mathbf{K} . Take the inertia moment of the strut I_4 as the study object. Let the inertia moment ratio be $\alpha = I / I_4$, where I is the inertia moment of the jib. As the process method elaborated previously, set $\xi \rightarrow \infty$ to simplify the investigation. The range of the inertia moment ratio is 0 to 10, the change curve between the ratio P_{cr} / P_E and the inertia moment ratio α is shown in Fig. 12.

As shown in Fig. 12, the buckling load drops with the increase of α , namely the decrease of the inertia moment I_4 . It should be pointed out that during the increase of α , i.e., the decrease of the inertia moment I_4 , there necessarily exists a critical point, from where the strut itself buckles before the overall buckling of the jib system. Therefore, there appears local buckling in the case of $\alpha \rightarrow \infty$, namely $I_4 \rightarrow 0$. As demonstrated in Fig. 12, the buckling load increases by about 17% when the inertia moment of the strut increases from $0.1I$ to ∞ .

4.4 The horizontal position of the cable fixed joint

The horizontal distance between the cable fixed joint and the hinge joint of jib 1 would influence the value of N_1 and N_4 directly. Recall Eq. (12), it can be seen that a_0 influences the transformation matrix \mathbf{R}_i , and thus influences the buckling characteristic equation. According to the notation method used in the Chinese design code for tower crane GB/T 13752 (2008), the length ratio between the length of jib segment 1 and the projection length of the jib cable 1 $\gamma = l_1 / a_1$ can be used to express the horizontal position of the cable fixed joint. It follows that $a_0 = (1 - 1 / \gamma) \cdot l_1$. Normally, the ratio γ is about 0.9 in the practical engineering. Therefore, it is reasonable to set the range of γ as 0.8~1.0. Similar to the preceding simplification, the lateral stiffness can be set infinite, the change curve between the critical compression ratio P_{cr} / P_E and the horizontal distance ratio γ can be obtained as shown in Fig. 13. Where P_E is the Euler critical compression $P_E = \pi^2 EI_1 / (2l_1)^2$.

As demonstrated in Fig. 13, the critical compression P_{cr} rises with the increase of the horizontal distance ratio γ . That is to say, there is a negative correlation between the buckling load of the jib system and the horizontal distance a_0 . Specifically, there appears a rise of about 7% for the buckling load during the increase of γ from 0.8 to 1.0, namely a_0 decreases from $0.25l_1$ to 0.

In conclusion, the horizontal distance a_0 is negatively correlated with the buckling load and its influence on the buckling load is slight.

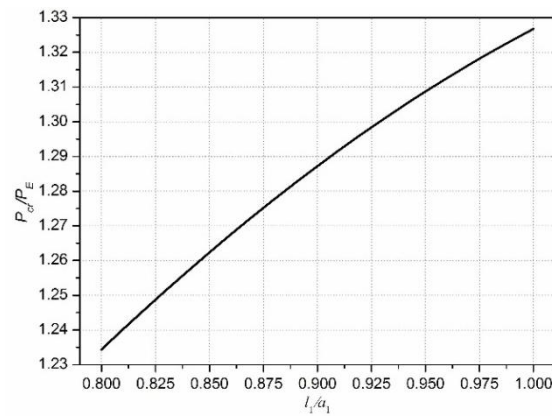


Fig. 13 The buckling load ratio along with the horizontal position of the cable fixed joint

5. Conclusions

The jib system with middle strut belongs to the tension structure. The existence of the strut leads to the flexural-torsional buckling mode. And the out-of-plane buckling analysis of the jib system becomes complicated, as there appears side sway combined with the torsional deformation. Aiming at the out-of-plane buckling behavior of the jib system, this paper established an accurate model accounting for the lateral flexibility of the cable fixed joint. Then, the bending and torsional differential equations of the jib system under the instability critical state were established. The analytical expression of the buckling characteristic equation was obtained by introducing the boundary conditions and deformation compatibility equations. Then the analytical solution was verified by the numerical solution presented by the widely used finite element software ANSYS.

A range of structural parameters were investigated to study their influences on the out-of-plane buckling behavior of the jib system. And the conclusions are as follows:

- The buckling load of the jib system increases with the rise of the lateral stiffness of the cable fixed joint. There is a significant rise for the buckling load when the lateral stiffness is relatively small, while the influence tends to be slight after the lateral stiffness reaches a certain level.
- The buckling load of the structure peaks when the dip angle of the strut is 90° . And the buckling load is larger when the dip angle is acute angle compared to that when the dip angle is obtuse angle.
- There is a positive correlation between the buckling load of the jib system and the inertia moment of the strut. And the influence is insignificant.
- The buckling load of the jib system is negatively correlated with the horizontal distance between the cable fixed joint and the jib hinge joint. And the influence is unremarkable.

Acknowledgments

This work was supported by National Natural Science Foundation of China (Grant No. 11172076) and Science and Technology Innovation Talent Foundation of Harbin (2012RFLXG020).

References

- De Araujo, R.R., De Andrade, S.A.L., Vellasco, P.D.S., Da Silva, J.G.S. and De Lima, L.R.O. (2008), "Experimental and numerical assessment of stayed steel columns." *J. Constr. Steel Res.*, **64**(9), 1020-1029.
- El-Ghazaly, H.A. and Al-Khaiat, H.A. (1995), "Analysis and design of guyed transmission towers — Case study in Kuwait", *Comput. Struct.*, **55**(3), 413-431.
- GB/T 13752 -2008 (2008), Design rules for tower crane; Standards Press of China, Beijing. [In Chinese]
- Hangai, Y. and Wu, M. (1999), "Analytical method of structural behaviours of a hybrid structure consisting of cables and rigid structures", *Eng. Struct.*, **21**(8), 726-736.
- Hosozawa, O., Shimamura, K. and Mizutani, T. (1999), "The role of cables in large span spatial structures: introduction of recent space structures with cables in Japan", *Eng. Struct.*, **21**(8), 795-804.
- Lan, P., Wang, T.F. and Lu, N.L. (2014), "Out-of-plane stability analysis for crane jib with single cable considering lateral flexibility of the cable fixed joint", *Proceedings of the 4th International Conference on Mechanical Engineering, Industry and Manufacturing Engineering*, Beijing, China, October.
- Li, W., Zhao, J., Jiang, Z., Chen, W. and Zhou, Q. (2015), "A numerical study of the overall stability of flexible giant crane booms", *J. Constr. Steel Res.*, **105**, 12-27.
- Lu, N.L., Wang, T.F. and Lan, P. (2014), "Calculation and analysis of whole stability in two hanging point horizontal arm rotation plane of tower crane", *Constr. Mach.*, **9**, 90-94. [In Chinese]
- Saito, D. and Wadee, M.A. (2009), "Buckling behaviour of prestressed steel stayed columns with imperfections and stress limitation", *Eng. Struct.*, **31**(1), 1-15.
- Timoshenko, S.P. and Gere, J.M. (1961), *Theory of Elastic Stability*, (2nd Edition), McGraw-Hill, New York, NY, USA.
- Wakefield, D.S. (1999), "Engineering analysis of tension structures: Theory and practice", *Eng. Struct.*, **21**(8), 680-690.
- Wang, T.F., Lan, P. and Lu, N.L. (2015), "Out-of-plane stability analysis of crane jib with auxiliary bracing", *Advanced Materials Research: Proceedings of 2014 International Conference on Machine, Energy, Chemistry and Applied-Information Technology*, Hefei, China, November.
- Wen, S.R., Lan, P. and Lu, N.L. (2013), "Stability analysis for horizontal boom with double pulling rods under non-conservative forces", *Proceedings of the 3rd International Conference on Mechanical Engineering, Industry and Manufacturing Engineering*, Wuhan, China, June.
- Wu, M. (2008), "Analytical method for the lateral buckling of the struts in beam string structures", *Eng. Struct.*, **30**(9), 2301-2310.
- Xue, W. and Liu, S. (2010), "Linear elastic and limit state solutions of beam string structures by the Ritz-method", *Struct. Eng. Mech., Int. J.*, **35**(1), 67-82.
- Yoo, H. and Choi, D.H. (2009), "Improved system buckling analysis of effective lengths of girder and tower members in steel cable-stayed bridges", *Comput. Struct.*, **87**(13), 847-860.